

Research on Braking Energy Regeneration for Hybrid Electric Vehicles

Mengtian Xu ¹, Jianxin Peng ^{1,2}, Xiaochen Ren ¹, Xuekun Yang ^{1,2} and Yuhui Hu ^{1,*}

¹ School of Mechanical Engineering, Beijing Institute of Technology, Beijing 100080, China

² Yangtze Delta Region Academy of Beijing Institute of Technology, Jiaxing 314000, China

* Correspondence: huyuhui@bit.edu.cn

Abstract: In recent years, there has been a significant increase in braking energy regeneration for hybrid electric vehicles. To improve performance and reduce fuel consumption, a better control strategy composed of braking regeneration and gear shifting is needed. This work presents a braking energy regeneration control strategy for a hybrid electric vehicle (HEV). The mathematical model for the vehicle dynamic system is established, and the objective function of braking energy regeneration is presented based on system analysis. Taking the increased electric energy of a battery as the objective function of the economic downshift law, the multi-island genetic algorithm (MIGA) is used to solve the shifting condition factors corresponding to different deceleration speeds and motor torques and the optimal downshifting speed. The presented control strategy of braking energy regeneration is validated in a typical city cycle form in China, and the results show better energy efficiency.

Keywords: shift schedule; hybrid electric vehicle (HEV); braking energy regeneration



Citation: Xu, M.; Peng, J.; Ren, X.; Yang, X.; Hu, Y. Research on Braking Energy Regeneration for Hybrid Electric Vehicles. *Machines* **2023**, *11*, 347. <https://doi.org/10.3390/machines11030347>

Academic Editors: Xianjian Jin, Chongfeng Wei, Chao Huang, Chuan Hu, Guodong Yin and Mohammed Chadli

Received: 26 December 2022

Revised: 7 February 2023

Accepted: 28 February 2023

Published: 3 March 2023



Copyright: © 2023 by the authors. Licensee MDPI, Basel, Switzerland. This article is an open access article distributed under the terms and conditions of the Creative Commons Attribution (CC BY) license (<https://creativecommons.org/licenses/by/4.0/>).

1. Introduction

Since the power source of a hybrid electric vehicle is combined with a motor and engine, there are three operation modes, which are the engine mode, hybrid mode, or integration in the control of the vehicle propulsion system with different driving situations [1,2]. Energy-saving for an HEV is very important due to the increasing requirements of fuel economy, driving performance, emissions, and safety. In recent years, more and more automatic transmissions have been installed in hybrid electric vehicles, and the above demands can be obtained via shift control with different control strategies, and, therefore, the energy-saving requirement of HEVs can be improved by changing different operation modes to integrate with shift control [3,4].

Many researchers have devoted themselves to the energy-saving requirement of HEVs. Based on the model predictive control algorithm, Ngo V made fuel burn more sufficiently under the engine starting energy loss effect by reducing the interruption of the AMT shifting process over time. An energy management strategy to achieve maximum fuel consumption efficiency could be obtained [5]. Hua Yuwei thought that reasonable torque split between the engine and motor could reduce transmission shift interruption. Speed regulating a motor can reduce shifting shock, and speed regulating an engine can reduce clutch wear and energy loss [6]. Qin Datong considered the efficiency of an engine and motor generator, a battery, and a transmission system, determining the working area of the driving conditions. The shift schedule of an HEV can be obtained in order to make the power source achieve the highest efficiency [7]. The present study on HEVs is mainly focused on the power and torque split algorithm between the engine and motor. This study is aimed at the starting or driving conditions, but the braking condition is not involved.

When an HEV is decelerating, an appropriate shifting speed and shift schedule are important to regenerate energy. Wang Weihua proposed that motor resistance torque, mechanical friction torque, and vehicle speed can be used as shifting parameters during braking to calculate the maximum regenerative energy, but this strategy ignores the

change in the motor torque in the process of shifting [8]. Liu Wenchao thought that both regenerative braking and friction braking based on fuzzy logic were assigned after the front-rear axle's braking force was distributed to meet the requirement of braking security and high-efficiency braking energy regeneration based on the characteristics of robustness in regenerative braking [9], but the influence of gear shifting on braking energy regeneration is not involved in the paper.

In this paper, the parameters (vehicle acceleration, motor torque, and weight of vehicle) that influence the process of regenerative braking energy were investigated. The optimal shifting velocity was decided via the maximum regenerative energy in the process of braking. To avoid frequent shifting, a control strategy was implemented when calculating the optimal shifting velocity.

Figure 1 shows the HEV platform propulsion system. It is a single-axle parallel hybrid electric vehicle that contains an engine, motor, clutch, battery, automated mechanical transmission (AMT), and a differential. The following work about system modeling, a braking control strategy, etc., is implemented based on this platform.

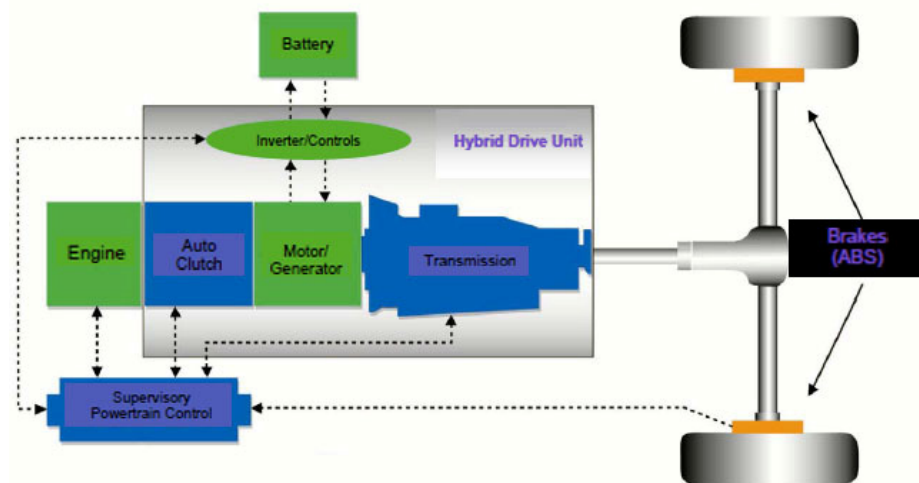


Figure 1. HEV propulsion system.

The parameters of the HEV are shown in Table 1.

Table 1. The parameters of HEV platform.

Component	Specification	Value	Unit
Engine	Type	Natural gas	-
	Rated power/speed	140/2500	kW/rpm
	Maximum torque/speed	650/1500	Nm/rpm
Motor	Type	Permanent magnet	-
	Rated power/speed	26/2600	kW/rpm
	Maximum torque/speed	420/1000	Nm/rpm
Battery	Voltage	360	V
	Capacity	8	Ah
Transmission	Gear ratio	7.05/4.13/2.52/1.59/ 1.00/0.78/R6.75	-

2. Mathematical Model and Objective Function

2.1. Vehicle System Model

The powertrain of the HEV includes an engine, clutch, motor, battery, transmission, differential, and wheels. Figure 2 shows the input and output of each system.

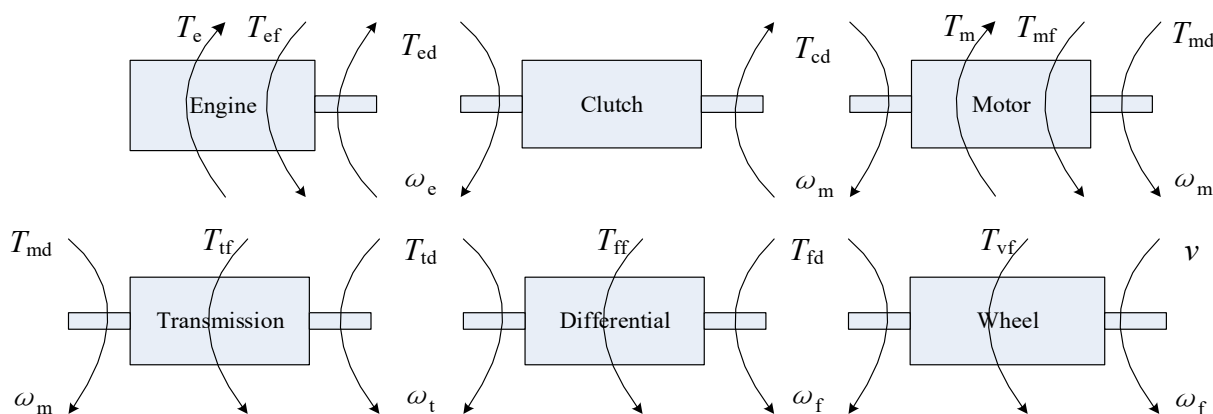


Figure 2. Input and output variables in dynamic system.

The vehicle dynamic model should be simplified to study the strategy of braking regeneration and gear shifting. The establishment of the model is based on these hypotheses [10,11]:

1. The torsional vibration of the engine and shaft and the effect of the clutch torsional damper on the system are neglected.
2. The transverse vibration of the drive shaft and the driven shaft is neglected.
3. Each component is a rigid inertial element without damping.
4. The clearance of the kinematic pair is neglected.

2.1.1. Engine Model

The engine model can be described as

$$J_e \dot{\omega}_e = T_e - T_{ef} - T_{ed} \tag{1}$$

where T_{ed} represents the output torque of the engine, T_e is the engine torque, T_{ef} is the internal friction torque, J_e is the inertia of the engine, and ω_e is the engine angular velocity.

The characteristics of the engine are acquired via test data, and the fitting curve of the characteristics is shown in Figure 3, and the polynomial fitting is shown in Equation (2).

$$T_e = 2.53 \times 10^{-7} n_e^3 - 1.54 \times 10^{-3} n_e^2 + 2.91 n_e - 1165.60 \tag{2}$$

where n_e is the engine speed.

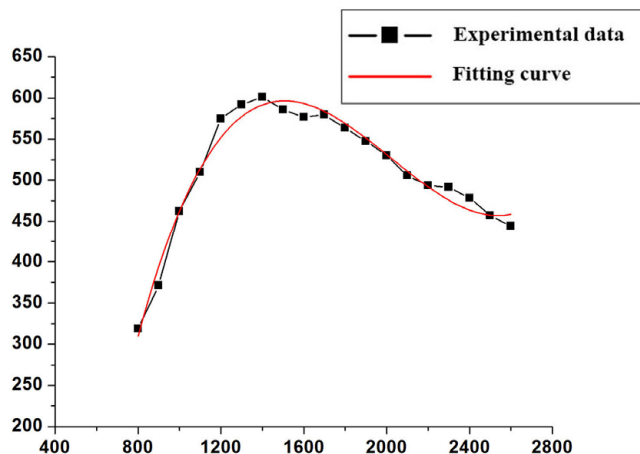


Figure 3. External characteristics of the engine and fitting curve.

2.1.2. Motor Model

The motor model is shown as

$$J_m \dot{\omega}_m = T_m - T_{mf} - T_{md} \tag{3}$$

The output torque of the engine is T_{md} . T_m is the engine torque, and T_{mf} is the internal friction torque of the engine. J_m is the inertia moment of the engine; ω_m is the motor angular velocity, where $\omega_m = \omega_e$.

The characteristics and working efficiency of the motor have a great influence on the energy regeneration of the hybrid electric vehicle. It is necessary to establish an accurate mathematical model for the motor via experimental tests. In this paper, the input and output of the motor are considered, and the external characteristics and the working efficiency of the motor are shown in Figure 4.

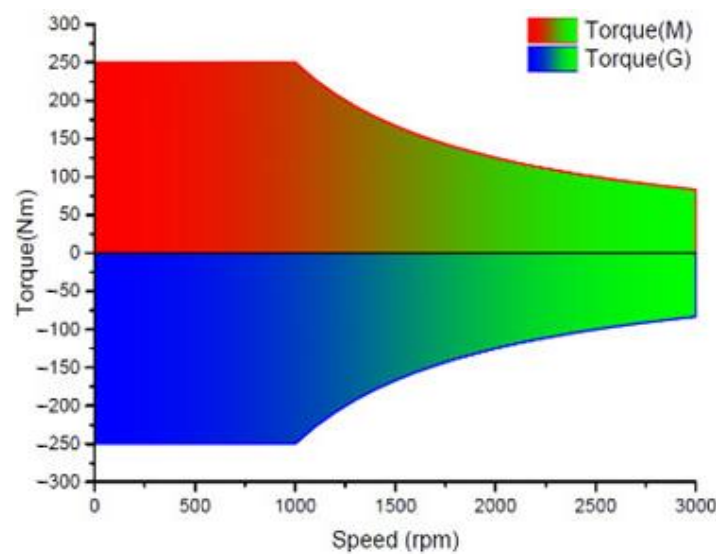


Figure 4. External characteristics and the working efficiency of the motor.

2.1.3. Battery Model

The SOC of the battery can be estimated in order to compare the consequence of the optimization strategy. The method is shown in Figure 5.

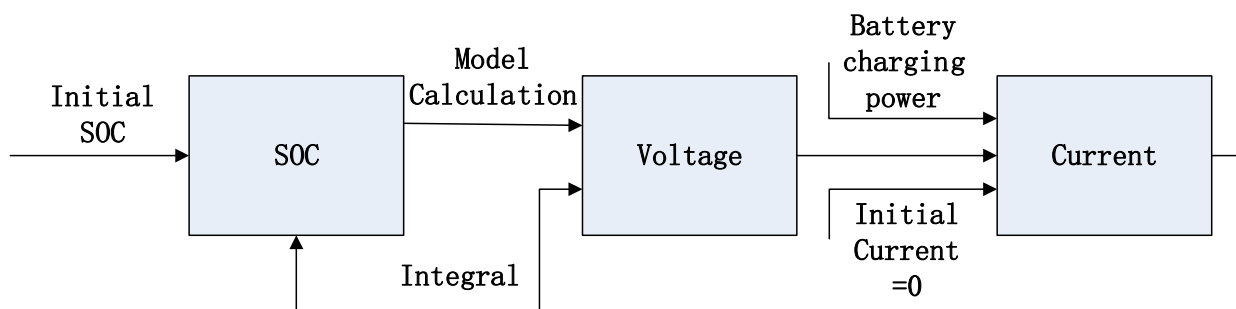


Figure 5. SOC estimation method.

The corresponding relationship between three parameters including the SOC and the voltage and current of the different vehicles is shown in Figure 6. The relationship between the three parameters is shown as (4). B_v is the voltage of the battery; B_c is the current of the battery; and B_s is the SOC of the battery.

$$B_v = 306.81 + 0.21B_c + 63.25B_s - 7.5 \times 10^{-5}B_c^2 - 6.44B_s^2 + 0.016B_sB_c \tag{4}$$

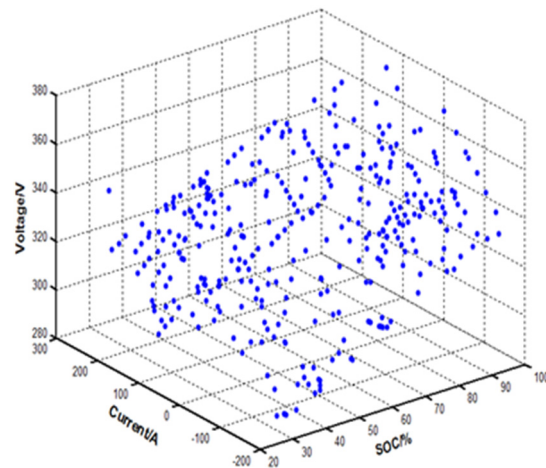


Figure 6. Corresponding relationship between three parameters.

The charging efficiency of a battery cannot be replaced by a fixed value because it is affected by many factors. The charging efficiency of the battery is shown in Figure 7.

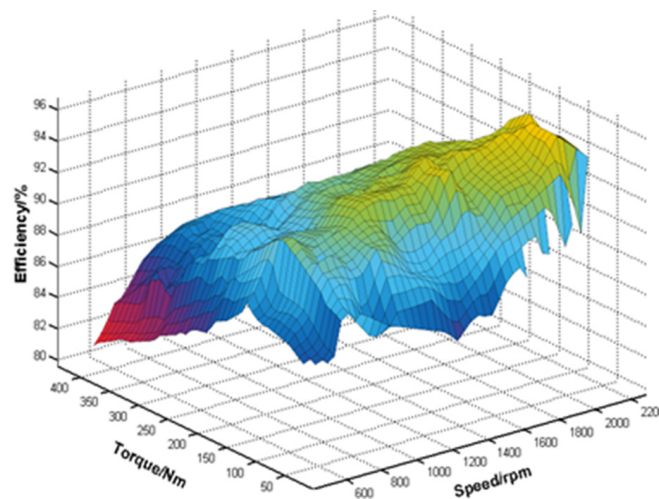


Figure 7. Charging efficiency of battery.

The effect of motor torque and speed on charging efficiency is analyzed with the DOE (design of experiment) method [12]. The charging efficiency coefficient of the electric machine for the battery is shown in Table 2. Furthermore, a secondary polynomial model for the charging efficiency of an electric machine for a battery can be expressed as (5).

$$\eta_{mb} = (0.0078n_m + 0.0229T_m - 2.07 \times 10^{-6}n_m^2 - 9.83 \times 10^{-5}T_m^2 + 1.03 \times 10^{-5}n_mT_m + 82.55)/100 \quad (5)$$

2.1.4. Other Mathematical Model

The clutch is assumed to be completely rigid when it is engaged; thus, the engine's rotary velocity is entirely equal to that of the input shaft's mechanical transmission [13].

If the transmission is in non-neutral gear, the output torque of transmission T_{td} should be expressed as (6). J_{t1} is the inertia moment of the input of transmission; J_{t2} is the inertia moment of the output of transmission; T_{tf} is the internal friction torque of transmission; and ω_t is the transmission output shaft angular velocity.

$$J_{t1}\dot{\omega}_m + J_{t2}\dot{\omega}_t = T_{md} - T_{tf} - T_{td} \quad (6)$$

Table 2. Table of charging efficiency coefficients.

	Coefficients	Scaled	Normalized
Constant	82.54907361		
n_m	0.007776876	3.796131489	31.01952404
T_m	0.022894698	−1.328832684	−10.8583587
n_m^2	$−2.07 \times 10^{-6}$	−1.49752163	−12.23677534
T_m^2	$−9.83 \times 10^{-5}$	−3.873657126	−31.65301326
$T_m - n_m$	1.03×10^{-5}	1.741735007	14.23232865

The dynamical equation of the final drive is expressed as (7). J_{f1} is the inertia moment of the input of the final drive; J_{f2} is the inertia moment of the output of the final drive; T_{ff} internal friction torque of the final drive; T_{fd} is the output torque of the final drive; and ω_f is the final drive angular velocity.

$$J_{f1}\dot{\omega}_t + J_{f2}\dot{\omega}_f = T_{td} - T_{ff} - T_{fd} \quad (7)$$

The vehicle dynamical model is expressed as (8). r is the wheel radius; m is the weight of the vehicle; g is gravitational acceleration; α is the road slope angle; C_D is the air resistance coefficient; A is the frontal area; v is the velocity of the vehicle; J_v is the inertia moment of the differential and wheel; a is the vehicle acceleration; f is the friction coefficient of the pavement; and α is the slope angle.

$$\frac{T_{fd}}{r} = mgf \cos \alpha + mg \sin \alpha + \frac{C_D A}{21.15} v^2 + ma + \frac{J_v \dot{\omega}_f}{r} \quad (8)$$

The whole vehicle dynamic equation can be simplified as (9). η_T is the mechanical efficiency of the transmission system; δ_i is the rotational mass conversion factor in i gear.

$$\frac{(T_{md} + T_{cd})i_i \eta_T}{r} = mgf \cos \alpha + mg \sin \alpha + \frac{C_D A}{21.15} v^2 + \delta_i ma \quad (9)$$

2.2. Objective Function

In the process of vehicle braking, the kinetic energy of vehicle loss needs to be regenerated as much as possible [14]. The change in the battery is taken as the objective function. If gear i has braking energy regeneration, and the change in the battery can be expressed as $R_{i,i-1}$, the function is shown as (10):

$$dR_{i,i-1} = \frac{T_m n_m \eta_{mb} \eta_b}{9549} dt \quad (10)$$

If the vehicle shifts gear in the process of braking, the shifting influence on energy regeneration should be considered. During downshifting, the motor should increase input speed and battery power. However, the unloading torque will charge the battery. To simplify the model, we assume that the SOC of the battery is unchanged. Moreover, the vehicle speed after downshifting can be expressed as

$$v_{sr} = v_s + 3.6a_b t_{br} \quad (11)$$

where v_s is the vehicle speed before downshifting; a_b is the downshifting acceleration; and t_{br} is the shifting time. In this paper, t_{br} is taken as 1.2 s, according to real vehicle experimental testing.

If the maximum speed in $i - 1$ gear is v_0 and the minimum regeneration speed in $i - 1$ gear is v_1 , the vehicle speed from v_1 to v_0 , the objective function of regeneration energy can be expressed as (12):

$$R_{i,i-1} = \int_0^{t_s} \frac{T_m n_m \eta_{mb} \eta_b}{9549} dt + \int_{t_s+t_{br}}^{t_1} \frac{T_m n_m \eta_{mb} \eta_b}{9549} dt = \int_{v_0}^{v_s} \frac{T_m n_m \eta_{mb} \eta_b}{9549 \times 3.6 \cdot a_i} dv + \int_{v_{sr}}^{v_1} \frac{T_m n_m \eta_{mb} \eta_b}{9549 \times 3.6 \cdot a_{i-1}} dv \quad (12)$$

If there is no gear shifting during the braking process, the objective function can be expressed as

$$R' = \int_{v_0}^{v_1} \frac{T_m n_m \eta_{mb} \eta_b}{9549 \times 3.6 \cdot a_i} dv \quad (13)$$

and in these two functions:

$$a_i = a_s - \frac{T_{ms} i_0 i_i \eta_t}{r \delta_i m} + \frac{T_m i_0 i_i \eta_t}{r \delta_i m}, a_{i-1} = a_s - \frac{T_{ms} i_0 i_{i-1} \eta_t}{r \delta_{i-1} m} + \frac{T_m i_0 i_{i-1} \eta_t}{r \delta_{i-1} m} \quad (14)$$

The optimal downshifting speed can be acquired through (12), and, whether shifting or not, we can compare the values of functions (12) and (13). The shifting objective function R can be shown as (15). If gear shifting is discontinuous, the parameter $i - 1$ can change to j ($j < i - 1$). The constraints of the engine, motor, battery, and transmission in the optimization process are to make sure that each component works in the allowed situation as (16).

$$R = \frac{\int_{v_0}^{v_s} \frac{T_m n_m \eta_{mb} \eta_b}{9549 \times 3.6 \cdot a_i} dv + \int_{v_s+a_b t_{br}}^{v_1} \frac{T_m n_m \eta_{mb} \eta_b}{9549 \times 3.6 \cdot a_{i-1}} dv}{\int_{v_0}^{v_1} \frac{T_m n_m \eta_{mb} \eta_b}{9549 \times 3.6 \cdot a_i} dv} \quad (15)$$

$$\begin{aligned} v_{\min,i-1} &\leq v_s \leq v_{\max,i-1} - 2 \\ v_{\min,i-1} &\leq v_s + 3.6 a_b t_{br} \leq v_{\max,i-1} - 2 \\ T_m n_m &\geq -P_{\max} \end{aligned} \quad (16)$$

3. Solving Process of the Optimization Problem

The optimization is based on an Isight and Matlab co-simulation [15,16].

The variables acceleration a_s , motor torque T_{ms} , and vehicle weight m in the objective function are sampled. To avoid the dispersion and accumulation of the sampling points, Latin hypercube sampling is used, and the consequences are shown in Figure 8.

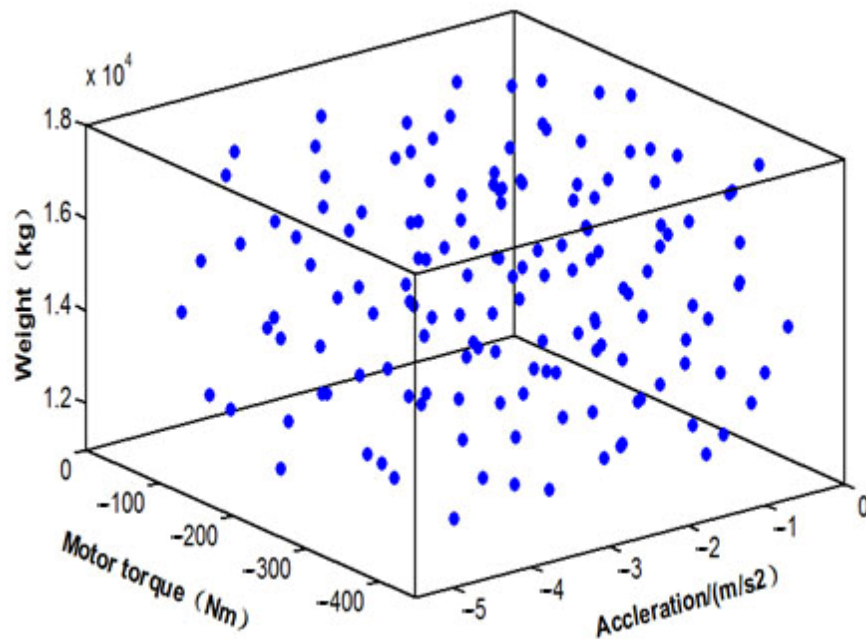


Figure 8. Latin hypercube sampling points.

Figure 9 shows the correlation diagram for the gear shifting condition factor r and optimal downshifting speed v_s .

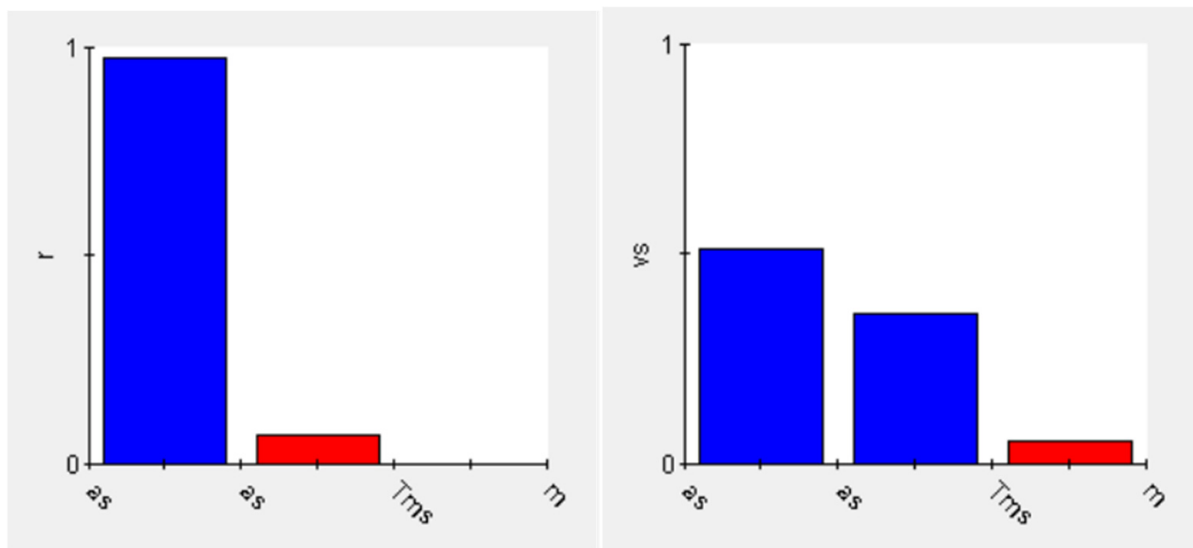


Figure 9. Correlation between shift condition factor and optimum downshifting speed.

As can be seen from Figure 9, the gear shifting condition factor r has the greatest correlation with speed reduction, and the correlation coefficient is very close to 1, followed by the motor torque during gear shifting, which has basically no correlation with vehicle weight. The optimal downshift speed v_s has a greater correlation with the speed reduction and motor torque but less correlation with vehicle weight.

Fuzzy control is used in the gear shifting schedule to avoid shifting frequently during the braking process. The objective function R is fuzzed, as shown in Figure 10.

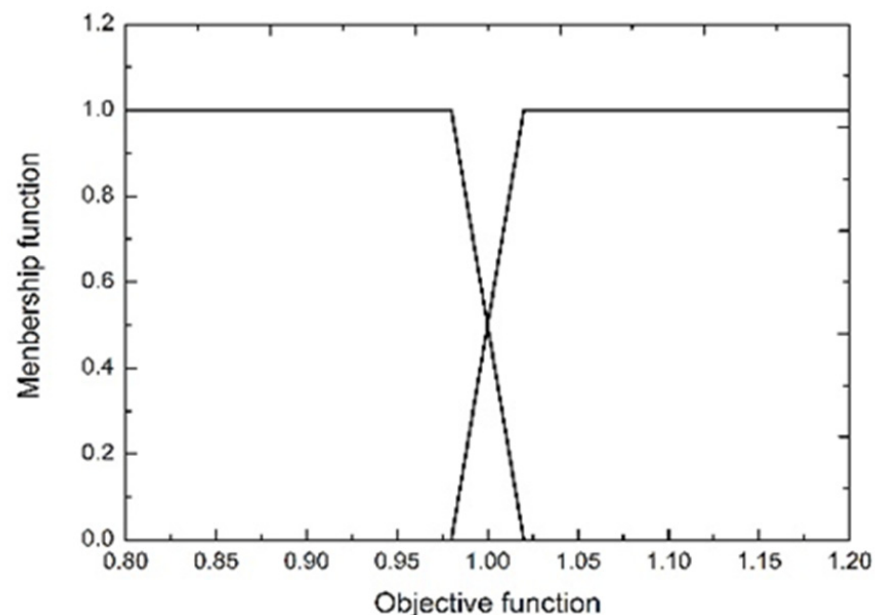


Figure 10. Membership function.

The gear shifting area is divided by two lines ($R = 0.98$ and $R = 1.02$). The area below the solid line is no gear shifting and above the dotted line is the shifting gear area. Moreover, between the solid line and the dotted line is the fuzzy control area, as shown in Figure 11.

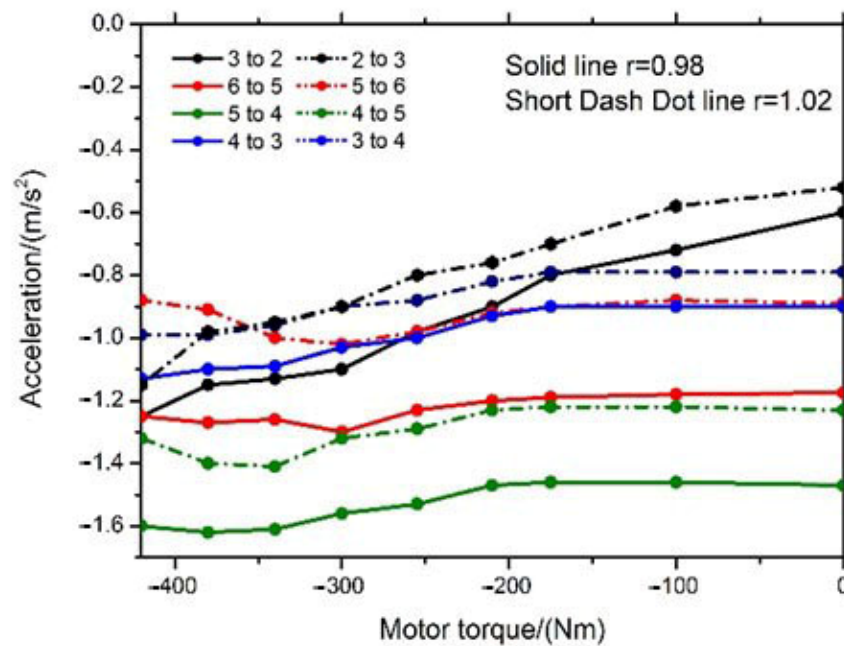


Figure 11. Gear shifting area division.

4. Optimization Results Analysis

The optimization results are shown in Figure 12.

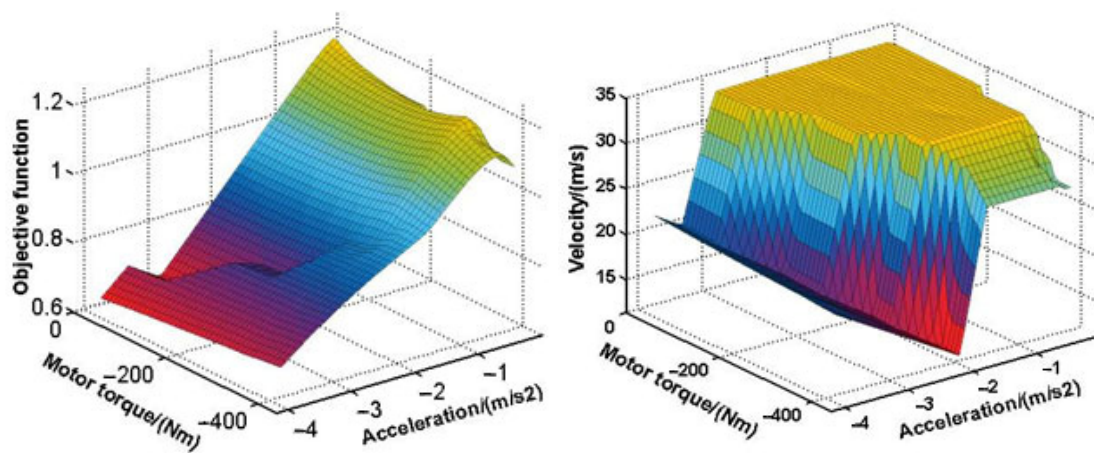


Figure 12. Gear shifting schedule in different gears (5 to 4).

However, the acceleration a_s and motor torque T_{ms} change during the braking process. If $r < 1$ at the beginning of braking, and with the changes in the acceleration a_s and motor torque T_{ms} , the objective function shows that the vehicle should shift, and the velocity of the vehicle is under the optimum downshifting velocity. Under this condition, the braking regeneration of the vehicle may not achieve maximum values. Thus, more studies should be conducted on this condition.

Over 1728 optimal points under different velocities are shown in Figure 13, and it shows that if the objective function $r > 1$ and the velocity of the vehicle is under the optimum downshifting velocity, with the increase in the velocity, the regeneration energy will increase. Furthermore, if the velocity of the vehicle is under the optimum downshifting velocity, the gear decision function is expressed as (17).

$$rr = \frac{\int_{v_2 - a_b t_{br}}^{v_1} \frac{T_m^{n_m} \eta_m \eta_b}{9549 \times 3.6 \cdot a_{i-1}} dv}{\int_{v_1}^{v_1} \frac{T_m^{n_m} \eta_m \eta_b}{9549 \times 3.6 \cdot a_i} dv} \tag{17}$$

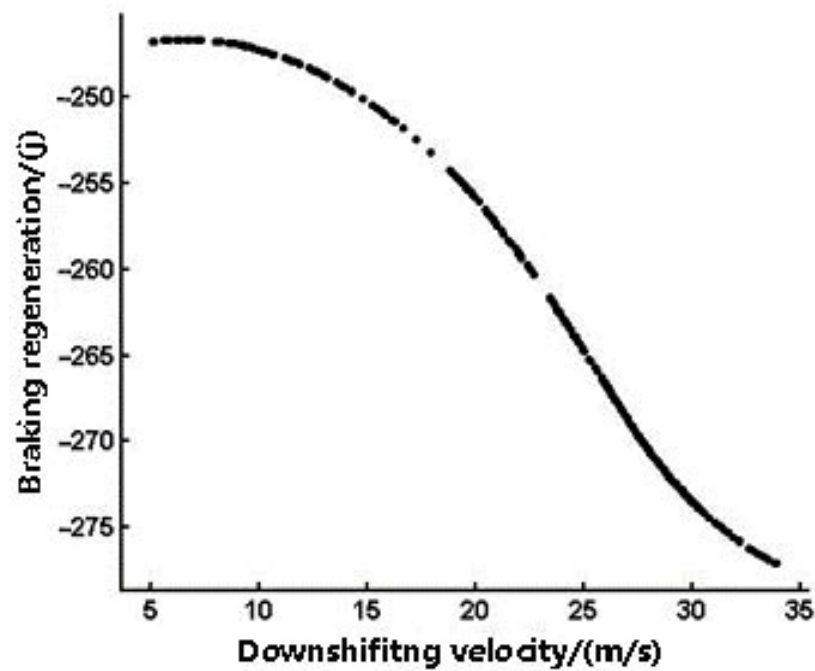


Figure 13. Braking regeneration energy under different downshifting velocities.

The three variables acceleration a_s , motor torque T_{ms} , and vehicle velocity v are sampled to calculate rr . These variables are discretized, as shown below.

$$\begin{aligned} a_s &\in \{-0.2, -0.4, -0.6, -0.8, -1, -1.2, -1.4\} \\ T_m &\in \{-20, -100, -180, -220, -260, -300, -340, -380, -420\} \\ v &\in \{6, 8, 10, 12, 14, 16, 18, 20, 22, 24, 26, 28, 30, 32, 34\} \end{aligned} \quad (18)$$

When $rr = 1$, the minimum vehicle velocity v_r can be obtained. Therefore, if the vehicle velocity v is lower than the minimum vehicle velocity v_r , there is no gear shifting. Moreover, if $v > v_r$, the vehicle shifts gear, and the optimization of the objective function can be shown as (19):

$$\text{Min } |rr - 1| \quad (19)$$

The consequence of the optimization of the vehicle velocity is shown in Figure 14.

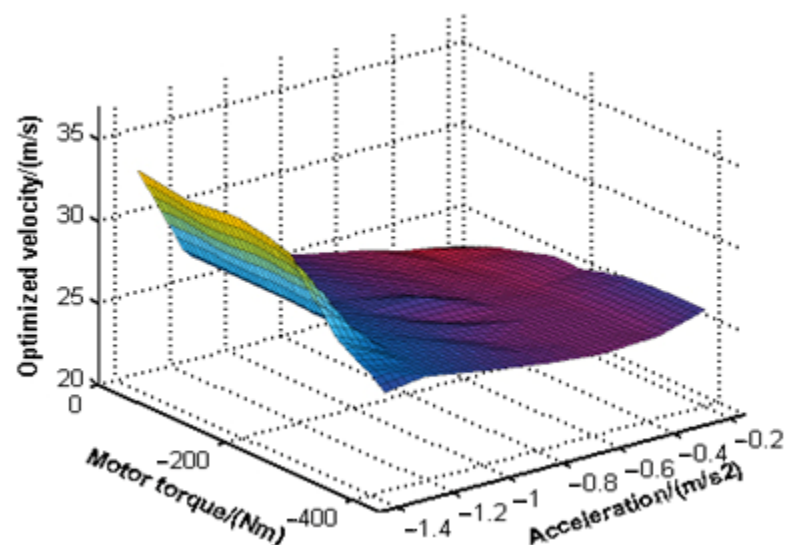


Figure 14. Optimization of vehicle velocity in gears 5 to 4.

5. Simulation and Validation of Optimization Results

5.1. Model Validation

Testing results are easily influenced by test conditions, and the comparison of equivalent fuel consumption between the platform and simulation is applied to validate the accuracy of the model. The typical urban driving cycle in China is shown in Figure 15. The real vehicle is shown in Figure 16.

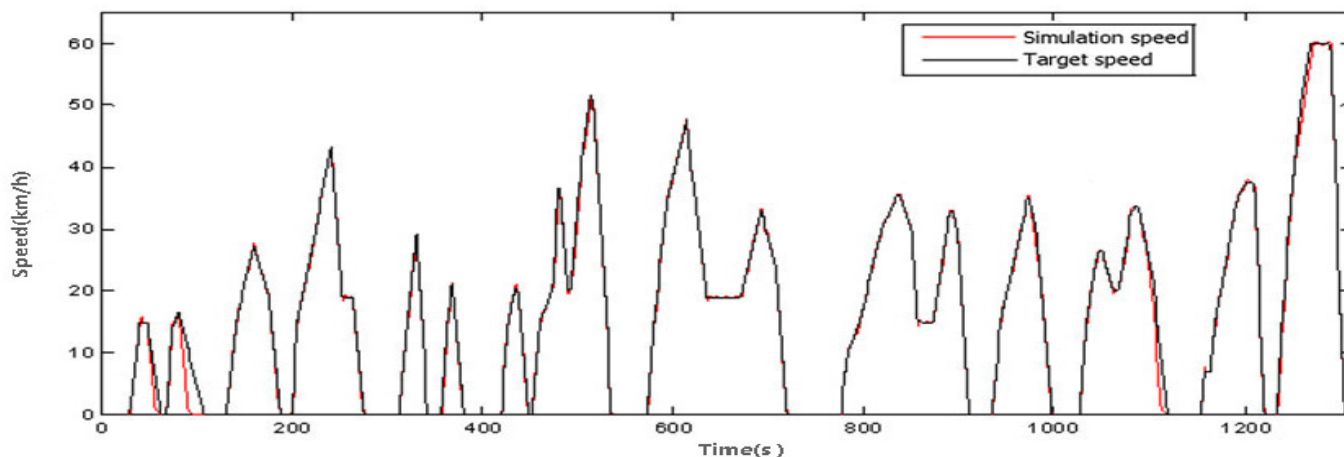


Figure 15. Typical Chinese urban driving cycle.



Figure 16. Hybrid electric vehicle.

The technical parameter list for this bus is shown in Table 3.

Table 3. Vehicle technical parameters.

Major Component	Main Parameter	Parameter Value
Engine	Output volume (L)	6.5
	Rated power/rotational speed (Kw/rpm)	140/2500
	Maximum torque/rotational speed (Nm/rpm)	650/1500
Clutch	Type	Single-piece dry-type diaphragm spring clutch
Motor	Type	Permanent magnet synchronous motor
	Voltage (V)	340

Table 3. Cont.

Major Component	Main Parameter	Parameter Value
Battery	Rated power/rotational speed (Kw/rpm)	26/2600
	Maximum torque/rotational speed (Nm/rpm)	420/1000
	Type	Aluminum–plastic film manganese oxide lithium-ion power battery
Transmission	Voltage (V)	360
	Capacity	8Ah
Transmission	Manipulation mode	AMT
	Speed ratio of each gear	7.05/4.13/2.52/1.59/1.00/0.78/R6.75

The vehicle model is established in AVL-Cruise and Matlab/Simulink, as shown in Figure 17.

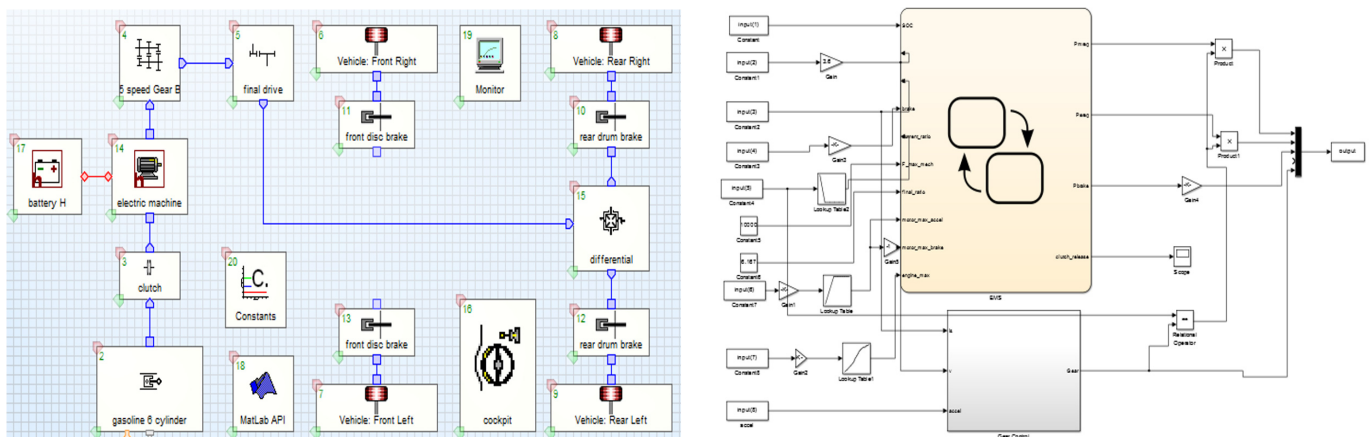


Figure 17. HEV model in Cruise and control strategy in Matlab/Simulink.

The instantaneous fuel consumption rate of the engine is delivered via a CAN message, as shown in Figure 18. The equivalent fuel consumption is made up of the changes in the SOC and the time integral of instantaneous fuel consumption. The result of the test bench is 32.60 L, and the simulation result is 33.16 L. There is only a 1.72% error between the two results, so the accuracy of the model can be accepted.

5.2. Validation of Gear Shifting Strategy in Braking Process

D gear is the economical driving gear, and in D gear, there is no shifting in the braking process. Gear shifting exists in low gear. Manual gear needs the driver to shift manually.

The vehicle model is established in Matlab/Simulink, and the simulation results are shown in Figure 19. The objective function varies between 0.8 and 1.6, and the energy of the recovery during the braking process makes the battery SOC increase by 0.544. Moreover, in low gear, the SOC increases by 0.538. In D gear, the vehicle does not shift gear during the braking process, and the SOC increases by 0.5. The optimization gear shifting strategy can save more than 8.1% of the regeneration energy.

5.3. Validation of Gear Shifting Strategy under Different Braking Strengths

The optimal downshifting strategy is taken into the simulation model. The starting braking speed is 70 km/h, and the different simulation results of the braking process with the shifting strategy, no shifting strategy, and optimization shifting strategy with different braking decelerations are shown in Table 4.

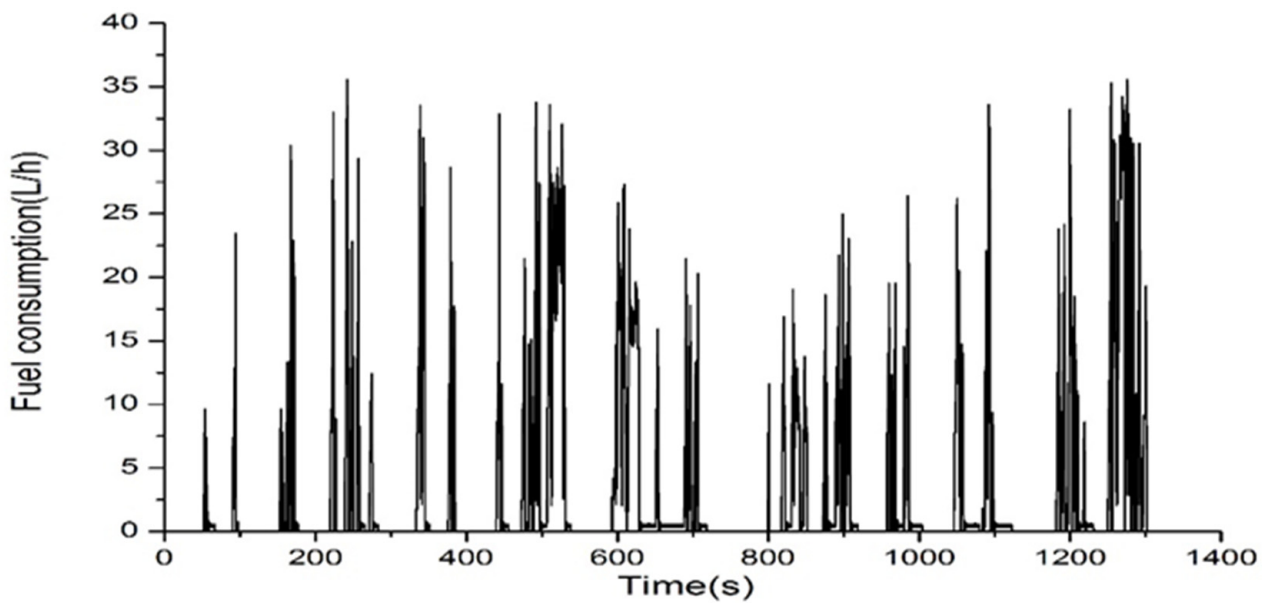


Figure 18. Instantaneous fuel consumption rate of engine.

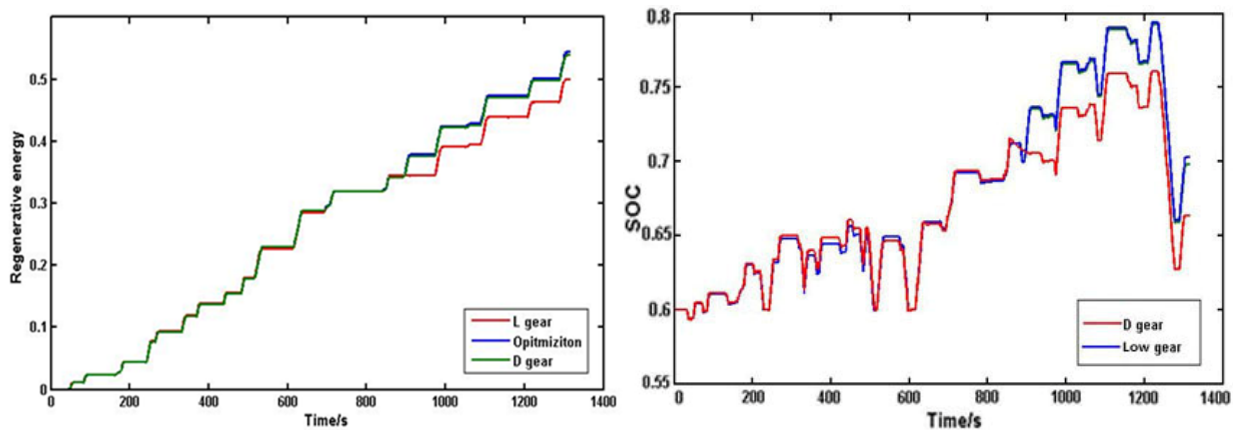


Figure 19. Simulation results.

Table 4. Different regeneration energy values under different braking strategies.

Acceleration (m/s ²)	Regeneration Energy			Acceleration (m/s ²)	Regeneration Energy		
	D	Optimal Strategy	L		D	Optimal Strategy	L
−0.4	0.1229	0.1229	0.1229	−1.2	0.0426	0.0439	0.0430
−0.5	0.0974	0.1022	0.1022	−1.3	0.0389	0.0391	0.0388
−0.6	0.0802	0.0843	0.0843	−1.4	0.0359	0.0359	0.0352
−0.7	0.0719	0.0758	0.0755	−1.5	0.0332	0.0332	0.0320
−0.8	0.0657	0.0691	0.0687	−1.6	0.0314	0.0314	0.0299
−0.9	0.0556	0.0581	0.0561	−2	0.0264	0.0264	0.0241
−1.0	0.0496	0.0515	0.0509	−3	0.0166	0.0166	0.0125
−1.1	0.0470	0.0498	0.0480	−4	0.0121	0.0121	0.0077

When the acceleration $a_s > 1.4 \text{ m/s}^2$, the optimal strategy is the same as D gear, and there is no gear shifting in the braking process. Compared with L gear, the optimal strategy braking energy regeneration increases from 3.8% to 57.4%. When the acceleration $a_s < 0.6 \text{ m/s}^2$, the optimal strategy is the same as L gear, and the vehicle should shift gear. Compared with D gear, the optimal strategy braking energy regeneration increases by approximately 5%. When the acceleration is $0.6 \text{ m/s}^2 < a_s < 1.4 \text{ m/s}^2$,

compared with D gear, the optimal strategy braking energy regeneration increases by approximately 0.5% to 5.3%. Compared with L gear, the optimal strategy braking energy regeneration increases from approximately 0.4% to 1.8%. From the above results, the optimal strategy appears to have a better performance in braking energy regeneration under different braking strengths.

6. Conclusions

In this paper, the braking downshifting decision and optimization method was investigated, and a shifting strategy was validated in a typical city bus cycle in China with different braking strengths. The results show that the optimal strategy appears to have a better performance in braking energy regeneration than D or L gear in a real vehicle.

Although the experimental platform of this paper is based on a single-axis parallel hybrid electric vehicle equipped with AMT, it is also suitable for a hybrid power system and other types of hybrid systems equipped with other types of transmission. Equivalent shifting times and transmission ratios for different transmission and control methods can be modified to make the shifting strategy suitable for AT and DCT. By modifying the objective function and the regenerative braking torque of the motor, the method of the shifting strategy can be applied to other types of hybrid systems.

Author Contributions: Conceptualization, Y.H.; Methodology, M.X.; Investigation, X.Y.; Data curation, X.R.; Writing—original draft, M.X.; Writing—review and editing, Y.H.; Supervision, J.P. All authors have read and agreed to the published version of the manuscript.

Funding: This research was partially supported by the National Natural Science Foundation of P. R. China (grant no. 51505029).

Institutional Review Board Statement: Not applicable.

Informed Consent Statement: Not applicable.

Data Availability Statement: Not applicable.

Conflicts of Interest: The authors declare no conflict of interest.

References

1. Berjoza, D.; Pirs, V.; Jurgena, I. Research into the regenerative braking of an electric car in urban driving. *World Electr. Veh. J.* **2022**, *13*, 202. [CrossRef]
2. Hu, X.; Johannesson, L.; Murgovski, N.; Egardt, B. Longevity-conscious dimensioning and power management of the hybrid energy storage system in a fuel cell hybrid electric bus. *Appl. Energy* **2015**, *137*, 913–924. [CrossRef]
3. Li, T.; Liu, H.; Zhang, Z.; Ding, D.-L. Shift scheduling strategy development for parallel hybrid construction vehicles. *J. Cent. South Univ.* **2019**, *26*, 587–603. [CrossRef]
4. Song, Q.; Ye, S.; Li, W. Research on AMT overall shift schedule for pure electric vehicles based on NSGA-II algorithm. *Chin. J. Automot. Eng.* **2017**, *7*, 44–51.
5. Ngo, V.; Hofman, T.; Steinbuch, M.; Serrarens, A. Effect of gear shift and engine start losses on energy management strategies for hybrid electric vehicles. *Int. J. Powertrains* **2015**, *4*, 141–162. [CrossRef]
6. Hua, Y. Research on Control Strategy for Double Synchronized Gear-Shift for Parallel Hybrid Electric Bus. Dalian University of Technology. 2014. Available online: https://kns.cnki.net/kcms2/article/abstract?v=3uoqIhG8C475K0m_zrgu4IQRvep2SAkVnKpVpjdBoadmPoNwLRuZyEhQbyUdN4bwC47MsOtZnyuqNqdK5mVILBfBvr8lzDA&uniplatform=NZKPT (accessed on 1 February 2023).
7. Qin, D.; Ye, X.; Hu, M.; Chen, Q. Optimization of Control Strategy for Medium Hybrid Electric Vehicle with ISG at Drive Condition. *J. Mech. Eng.* **2010**, *46*, 86–92. [CrossRef]
8. Wang, W.; Wang, Q.; Zeng, X. Research on Gear-shift Schedules in the Braking Process of Parallel Hybrid Electric Bus. *J. Jilin Univ.* **2009**, *39*, 10–13.
9. Liu, W.; Chen, G.; Zong, C.; Li, C. Research on Electric Vehicle Braking Force Distribution for Maximizing Energy Regeneration. In Proceedings of the SAE 2016 World Congress and Exhibition, Detroit, MI, USA, 12–14 April 2016.
10. Lu, J. *Hill-Start Control Strategy of Heavy Off-Road Vehicles Equipped with AMT Based on Multi-Signal Integration*; Beijing Institute of Technology: Beijing, China, 2014.
11. Guo, H. *Optimization Study on Control Strategy for the Cooperative Braking System in an Electric Vehicle with Independently Driven Front and Rear Axles*; Beijing Institute of Technology: Beijing, China, 2014.

12. Shen, W.; Hu, Y.; Yu, H. Shifting Process Control of AMT Based on Virtual Clutch Technology for Hybrid Electric Vehicle. *J. Mech. Eng.* **2014**, *50*, 108–117. [[CrossRef](#)]
13. Mehrdad, E.; Yinin, G.; Ali, E. *Modern Electric, Hybrid Electric, and Fuel Cell Vehicles: Fundamentals Theory, and Design*, 2nd ed.; CRC Press: Boca Raton, FL, USA, 2010.
14. Lai, Y.; Jiang, X.; Fang, L. *Optimization Theory and Examples of Parameters by Isight*; Beihang University Press: Beijing, China, 2012.
15. Zhong, Y.; Chen, B.; Wang, Z. *Principles and Methods of Multidisciplinary Design Optimization*; Huazhong University of Science and Technology Press: Wuhan, China, 2007.
16. Yu, Z. *Automobile Theory*; Machinery Industry Press: Beijing, China, 2019.

Disclaimer/Publisher's Note: The statements, opinions and data contained in all publications are solely those of the individual author(s) and contributor(s) and not of MDPI and/or the editor(s). MDPI and/or the editor(s) disclaim responsibility for any injury to people or property resulting from any ideas, methods, instructions or products referred to in the content.